Functional Layers for Zn−II Ion Detection: From Molecular Design to Optical Fiber Sensors

ARTICLE *in* THE JOURNAL OF PHYSICAL CHEMISTRY B · DECEMBER 2013

Impact Factor: 3.3 · DOI: 10.1021/jp407460c · Source: PubMed

THE JOURNAL OF PHYSICAL CHEMISTRY B

Article

pubs.acs.org/JPCB

Functional Layers for Zn^{II} Ion Detection: From Molecular Design to Optical Fiber Sensors

Zhihong Liu,[†,‡,∥] Claire Tonnelé,[*,§,∥] Glauco Battagliarin,[†] Chen Li,[†] Radu A. Gropeanu,[†] Tanja Weil,[†,#] Mathieu Surin,[§] David Beljonne,[§] Roberto Lazzaroni,[§] Marc Debliquy,[⊥] Jean-Michel Renoirt,[⊥] and Klaus Müllen[†]

[†]Max Planck Institute for Polymer Research, Ackermannweg 10, D-55128 Mainz, Germany

[‡]Qingdai Institute of Bioenergy and Bioprocess Technology, Chinese Academy of Sciences, 266101 Qingdao, China

[#]Department of Chemistry, National University of Singapore, 3 Science Drive 3, Singapore 117543, Singapore

[§]Laboratory for Chemistry of Novel Materials and [⊥]Service de Science des Matériaux, University of Mons-UMONS, Place du Parc 20, 7000 Mons, Belgium

Supporting Information

ABSTRACT: We report on the synthesis of a novel perylene monoimide derivative that shows high response and selectivity for zinc ion detection. The complexation of Zn^{2+} by the dye is followed by FD-MS, ^1H NMR, UV−vis spectroscopy, and isothermal titration calorimetry. Quantum chemical calculations are performed to gain further insight into the electronic processes responsible for the spectroscopic changes observed upon complexation. Finally, the perylene dye is incorporated in a sol−gel silica layer coated on optical fibers that are then used for Zn^{2+} detection in aqueous solution.

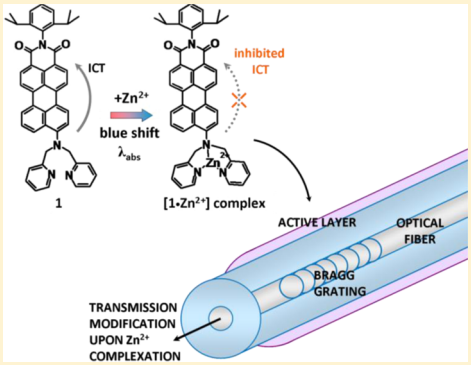

INTRODUCTION

Nowadays, zinc is one of the most heavily consumed metals in the industry, with numerous applications such as in alloys, in particular, for corrosion protection of steel, oxide fillers, and batteries. Its widespread use has raised the need for Zn^{2+} chemosensors, and the development of probes for the zinc ion in water has retained much interest in the past decade.[1]

The possibility to efficiently custom design the molecular structure of organic dyes according to needs provides a cheap and straightforward platform for the creation of efficient optical sensors. Most organic-based optical probes rely either on inter/intramolecular photoinduced electron transfer (PET),[2−4] or on charge transfer.[5] The former usually consists of a chromophore−spacer−receptor system that undergoes fluorescence quenching or enhancement in the presence of the analyte, while the latter involves a conjugated chromophore−receptor pair and relies on ratiomeric sensing using either light absorption or emission. Among all of the available chromophores, perylene dyes are widely used in commercial applications due to their outstanding chemical, thermal, and photochemical stability, their low toxicity, and low cost.[6−14] These features make them attractive building blocks for the design of novel intramolecular charge transfer (ICT) chemosensors. The implementation of such sensing molecules on optical fibers opens the way to a new type of chemical sensors with enhanced capabilities (small size, lightweight, flexibility, distributed sensing).[15]

In this work, we describe the synthesis of *N*,*N*-bis(2-picolyl)-9-aminoperylene monoimide (PMI) (**1**) as a molecular dye for Zn^{2+} sensing. FD-MS, ^1H NMR, and UV−vis spectroscopy as well as isothermal titration calorimetry were performed to characterize the PMI−Zn^{2+} complex and demonstrated the highly responsive and selective sensing for Zn^{2+}. Quantum chemical calculations were carried out to provide a molecular picture for the spectroscopic response observed upon complexation of Zn^{2+}. The ability to sense zinc ions in solution was demonstrated in thin films of **1** on glass. Finally, an optical fiber sensor was fabricated by encapsulation of **1** in a microporous sol−gel grown on the fibers as the sensitive element, proving the validity of our approach for the facile detection of zinc ions in water.

EXPERIMENTAL SECTION

Synthesis. *N*-diisopropylphenyl-9-bromoperylene-3,4-monoimide (200 mg, 0.357 mmol), di-(2-picoly)amine (106 mg, 0.537 mmol), tris(dibenzylideneacetone)dipalladium(0) (60 mg, 0.066 mmol), tris-*tert*-butylphosphine (20 mg, 0.09 mmol), sodium-*tert*-butoxide (67 mg, 0.69 mmol), and dry

Received: July 26, 2013
Revised: December 5, 2013
Published: December 11, 2013

Scheme 1. Synthesis of 1[a]

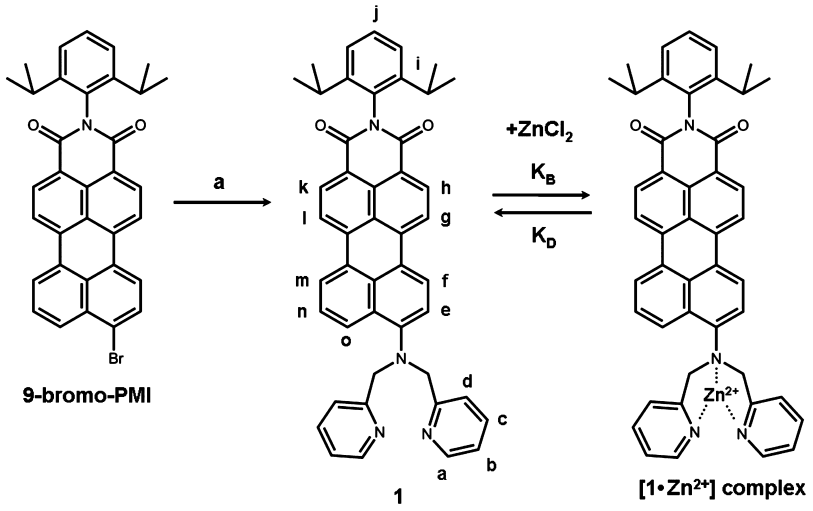

[a]Conditions: (a) bis(2-picolyl)amine, tris(dibenzylideneacetone)dipalladium(0) ($Pd_2(dba)_3$), tris-*tert*-butylphosphine, *t*-BuONa, toluene, 80 °C, 12 h; yield: 50%.

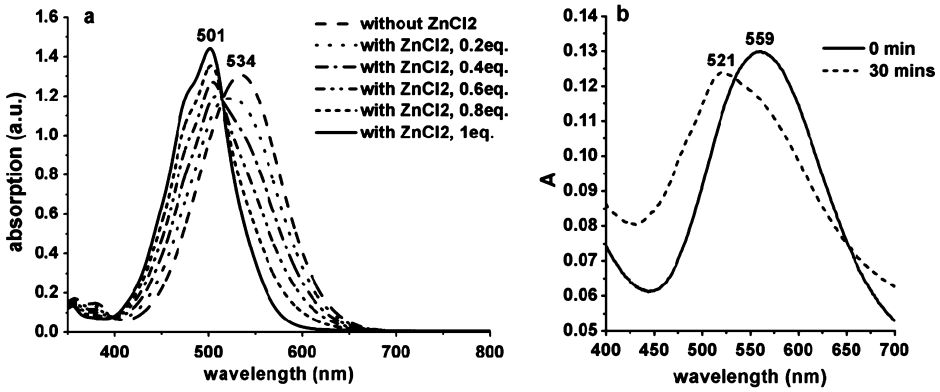

Figure 1. (a) Absorption spectra of the complexes of **1** (4.42×10^{-5} M) with increasing amounts of $ZnCl_2$ in acetone solution. (b) Absorption spectra of a film of **1** dipped in an aqueous solution of Zn^{2+} (2.0 M) at t = 0 and 30 min.

toluene (20 mL) were stirred at 80 °C under argon overnight. After cooling, the mixture was evaporated in vacuo and purified by column chromatography on silica gel using dichloromethane/acetone (4:1, v/v) as an eluent. The 120 mg of clean product was obtained as a violet solid in a 50% yield. ^{1}H NMR (250 MHz, CD_2Cl_2, 25 °C): δ = 8.68(d, J = 8.3 Hz, 1H), 8.56−8.45(m, 3H), 8.41(d, J = 8.0 Hz, 2H), 8.32(d, J = 8.3 Hz, 1H), 8.13(d, J = 8.3 Hz, 2H), 7.63−7.50(m, 3H), 7.43−7.37(m, 3H), 7.27(d, J = 7.9 Hz, 2H), 7.16−7.06(m, 3H), 4.59(s, 4H), 2.73−2.61(sep, J = 6.9 Hz, 2H), 1.09−1.07 ppm (d, J = 6.9 Hz, 12H). ^{13}C-NMR (62.5 MHz, CD2Cl2, 25 °C): δ = 162.6, 156.7, 149.2, 147.9, 144.7, 136.5, 130.4, 129.2, 128.2, 127.9, 125.7, 125.0, 123.1, 122.9, 120.9, 119.2, 118.1, 117.6, 58.4, 27.6, 22.2 ppm. IR: ν = 3060, 2960, 2930, 2860, 1690, 1650, 1560, 1500, 1350, 1290, 1240, 1210, 1130, 843, 804 cm^{-1}. MS (FD): m/z 678.2(100%) M+.

Optical Fibers. The gratings were fabricated into hydrogen-loaded single-mode standard silica fibers with UV laser light at 244 nm. The external tilt angle was set to 6° with a grating length of 8 mm.

The sensitive sol−gel coating was obtained by incorporation of the dye in a sol−gel solution (1 wt %). The sol−gel solution was prepared by mixing ethanol (15 mL), tetraethoxysilane (TEOS) as the precursor (15 mL), water (3 mL), and HCl as the catalyst for the sol−gel formation (2 M, 0.25 mL). The solution was heated at 60 °C (reflux) for 1 h and aged for 1 week before use.

The sensitive layer was deposited along the fiber by dip coating in one step and annealed at 80 °C for 1 h in air (35% relative humidity), yielding a 5 μm thick transparent purple layer. The amplitude transmission spectra of the sensors were measured using a nonpolarized source (Ammonics) in the 1520−1580 nm range and an optical spectrum analyzer (Ando AQ6317C). The spectrum was measured in about 60 s. The fibers were immersed in a 1 M NaCl solution, and the Zn^{2+} concentration was adjusted to 1 M by adding $ZnCl_2$. NaCl was introduced to ensure that the refractive index of the solution was not affected (as controlled with a refractometer).

Quantum Chemical Calculations. The ground-state geometry of **1** in the absence/presence of Zn^{2+} was optimized at the density functional theory B3LYP/6-31G* level.[16] Those equilibrium geometries were subsequently used as input for the calculation of the electronic excited states and the simulation of the optical absorption spectra in the framework of time-dependent density functional theory (TD-DFT). We used the LanL2DZ[17] effective core potential and a valence basis set to describe the zinc ion. Solvent effects were taken into account by combining a dielectric continuum model (IEFPCM[18]) with an

dx.doi.org/10.1021/jp407460c | J. Phys. Chem. B 2014, 118, 309−314

explicit description of the first solvation shell by acetone molecules. Static isotropic molecular polarizabilities were computed at the B3LYP/6-31+G(d) level from the previously optimized geometries by solving the coupled perturbed Hartree−Fock equations. All of the calculations were carried out using the Gaussian (G09) program package.[19]

RESULTS AND DISCUSSION

The synthesis of *N*-(2,6-diisopropylphenyl)-*N*′,*N*′-bis(2-picoly)-9-aminoperylene-3,4-dicarboximide (**1**) was achieved via a one-step reaction in 50% yield by palladium-catalyzed coupling of 9-bromo-PMI with bis(2-picolyl)amine under Buchwald conditions (Scheme 1).[20,21] The product was fully characterized by ^{1}H NMR, ^{13}C NMR, and FTIR spectroscopy, as well as elemental analysis (see the Supporting Information (SI)).

Compound **1** exhibits an absorption maximum at 534 nm in acetone and an hypsochromically shifted peak at 501 nm in the presence of 1 equiv of $ZnCl_2$, with a clear isosbestic point at 515 nm (Figure 1a), consistent with a transition from purple (i.e., the color of **1**) to red (a color similar to PMI without substitution in the 9 position). The fluorescence maximum shifts from 702 nm (Φ = 0.21) without Zn^{2+} to 670 nm (Φ = 0.36) with 1 equiv of Zn^{2+} (see the SI, Figure S1) as a consequence of the **1**·Zn^{2+} complex formation. The pronounced modifications in fluorescence maxima and quantum yields between **1** and **1**·Zn^{2+} reflect a significant Zn^{2+}-dependent color change, which can easily be observed even without the use of a spectrophotometer.

Both FD-MS and ^{1}H NMR spectroscopies clearly confirm the formation of the **1**·Zn^{2+} complex. The ^{1}H NMR data show the change of chemical shifts of the protons H_a, H_b, and H_c (Scheme 1) at the pyridine rings, where the signals are changed from 8.59, 7.24, and 7.77 ppm to 9.41, 7.82, and 8.13 ppm, respectively, in the presence of 1.0 equiv of $ZnCl_2$ (see the SI, Figure S3). This can be explained by the fact that the electron density at C_a, C_b, and C_c in the pyridine rings is decreased when Zn^{2+} is complexed by the pyridinic nitrogen atoms.

Isothermal titration microcalorimetry (ITC) represents a valuable experimental method in the determination of the thermodynamic parameters characterizing recognition processes.[22] Figure 2 shows the result of a typical ITC titration experiment of **1** with $ZnCl_2$. The upper graph presents the raw data (heat flow versus time) for the addition of small portions of a 570 μM $ZnCl_2$ solution to bis(picolyl)-PMI **1** (44 μM). In the beginning of the titration, the observed heat change is mainly due to dilution of the zinc salt and to the $[\mathbf{1}\cdot Zn]^{2+}$ complex formation, while at the end of the experiment, only the heat of dilution is detected. Each peak of the raw data was integrated and plotted against the $ZnCl_2$/**1** molar ratio. To eliminate the influence of $ZnCl_2$ dilution on the measurement, a separate titration, which consisted of injection of the salt into the pure solvent under the same conditions as those in the complexation experiment, was performed. After subtraction of the $ZnCl_2$ dilution, the normalized heat curve (Figure 2, lower panel) was fitted to a standard 1:1 model to calculate ΔH, ΔS, K_D, and ΔG (Table S1, SI). The complexation of Zn^{2+} with **1** in acetone was detected as an endothermic process with a moderate positive enthalpy (4.7 kcal/mol). The unfavorable enthalpy is compensated by a higher entropic term ($T\Delta S$ = 12.0 kcal/mol), rendering the Gibbs energy negative (−7.3 kcal/mol). The complexation stoichiometry determined by ITC was approximately 1:1, which correlates with the UV−vis

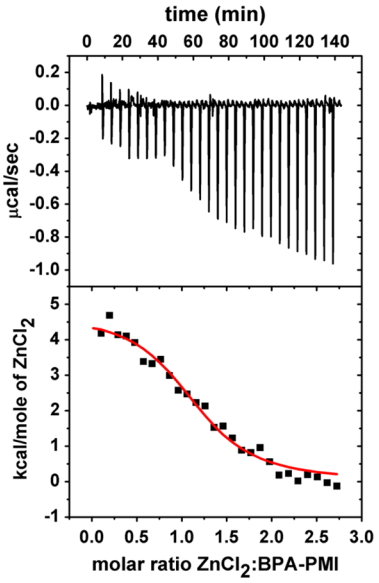

Figure 2. Titration of **1** (44 μM) with a 570 μM solution of $ZnCl_2$ in acetone at 25 °C. (Upper panel) Raw titration curve. (Lower panel) Corrected heats for each injection and correlation (red line).

data. The calculated dissociation constant (K_D, Scheme 1) of $[\mathbf{1}\cdot Zn]^{2+}$ is in the micromolar range ($K_D = 5 \times 10^{-6}$ mol/L).

The sensitivity of **1** to other cations, Ca^{2+}, Ag^{+}, Hg^{2+}, Fe^{2+}, Cu^{2+}, Ni^{2+}, and Co^{2+} (from aqueous solutions of $CaCl_2$, $AgNO_3$, $HgCl_2$, $FeCl_2$, $CuCl_2$, and $NiCl_2$, respectively), was also investigated. None of the equimolar complexes of **1** with the above-mentioned cations resulted in fluorescence enhancement at 600 nm under irradiation at 515 nm (see the SI, Figure S5), in contrast to the results for the Zn^{2+} ion. The Hg^{2+} ion generated a negligible two-fold increase of compound **1** fluorescence as compared to the fluorescence enhancement induced by Zn^{2+} (20-fold increase). Note that (i) we chose to monitor the emission intensities at 600 nm, rather than at the 670 nm maximum, because of a more favorable signal-to-noise ratio, (ii) Cu^{2+} quantitatively quenches the fluorescence due to the PET already demonstrated by others, and (iii) these experiments do not account for the competitive binding of different ions that would be simultaneously present in solution.[23]

Quantum chemical calculations were performed to get insight into the detection mechanism of Zn^{2+} complexation observed in solution and semiquantitatively predict the subsequent refractive index changes, which are relevant for fiber sensing. In the absence of Zn^{2+}, the calculated absorption spectrum from the optimized ground-state geometry of **1** (see the SI, Figure S7a) presents an absorption band at ∼555 nm associated with an excited state largely dominated by the HOMO/LUMO transition. Though slightly underestimated (∼21 nm or ∼0.1 eV), the computed transition energy can be considered in good agreement with the experimental value measured in acetone.

Optimization of the PMI−Zn^{2+} system yields two different local minima with relatively close energy (∼0.39 eV). In the first conformation (noted a hereafter), the zinc ion interacts only with the two pyridinic nitrogen atoms, whereas a larger conformational rearrangement brings the ion closer to the nitrogen atom on the 9 position (N9) in the more stable conformation (noted b; see the SI, Figure S7b). In both cases, the coordination shell of Zn^{2+} appears incomplete, suggesting

dx.doi.org/10.1021/jp407460c | J. Phys. Chem. B 2014, 118, 309−314

that at least one additional ligand, such as one acetone molecule interacting via its oxygen atom, could also bind the metal ion. To investigate the relative stability and spectroscopic properties of complexes characterized by different coordination numbers (CNs) of Zn^{2+} (namely 4, 5, and 6), explicit acetone molecules were added to the system. All geometry optimizations yield stable structures, except CN = 6 in **1b** because of too large steric hindrance.

Two acetone molecules were included in the system in **1a** to obtain the (distorted) tetrahedral geometry of the tetra-coordinated complex (see Figure 3). The simulated absorption

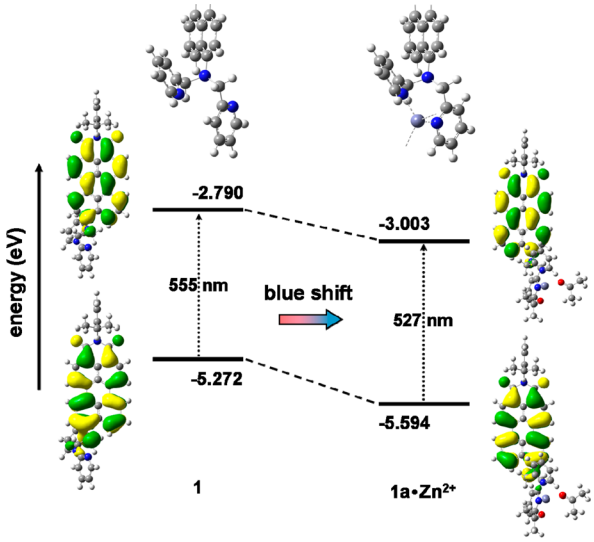

Figure 3. Evolution and graphical representation of the frontier orbitals of **1** upon complexation of Zn^{2+}. Only the terminal part of the rylene unit and the two pyridine rings are shown in the molecular structures, for the sake of clarity.

spectrum of **1a**·Zn^{2+} presents a strong absorption band at ~527 nm corresponding to the $S_0 \rightarrow S_1$ transition, which essentially corresponds to a HOMO → LUMO excitation, as found in the free molecule. The computed blue shift of the first absorption band upon complexation amounts to ~28 nm and comprises two different contributions, a conformational reorganization and a change in the electronic structure. The main structural modification in the presence of the ion involves the rotation of one pyridine unit in the ionophore. To assess this effect, we have computed the absorption spectrum of the complex in its equilibrium geometry, after removal of the zinc ion and acetone molecules, to isolate the conformational rearrangement. It is found to provide only a ~3 nm contribution to the hypsochromic shift, which is thus dominated by electronic effects (see the discussion below). Note that the same conclusions can be drawn for the other CNs investigated (5 and 6).

1b is characterized by a larger torsion angle around the perylene ionophore C–N bond, together with a shorter distance between Zn^{2+} and N9, suggesting a stronger electronic interaction and, as a result, a stronger impact on the absorption spectrum compared to that of **1a**.

In line with these expectations, the simulated absorption spectrum of **1b**·Zn^{2+} + one acetone molecule (CN = 4) shows a more pronounced blue shift (compared to **1a**·Zn^{2+}); the lowest optical transition (mainly HOMO → LUMO) is computed at ~504 nm, hypsochromically shifted by ~51 nm with respect to the free dye. Of this shift, a ~14 nm contribution stems from conformational effects. Structure CN = 5 obtained by adding a second solvent molecule shows the same behavior.

In all structures investigated, the quantum chemical calculations indicate that addition of Zn^{2+} to the perylene dye entails a blue shift of the lowest absorption band, qualitatively and quantitatively in agreement with the experimental spectroscopic data in solution and in the films (see below). Focusing on the electronic structure, we notice that the formation of the complex is accompanied by an asymmetric stabilization of the frontier molecular orbitals that are mostly involved in the lowest electronic excitation, with a larger lowering of the HOMO, resulting in the overall blue shift (Figure 3). This effect is due to a reduced electronic density over the nitrogen atom in the 9 position (thereby reducing its electron-donating strength) and a concomitant smaller ICT character of the amino-substituted PMI dye in the presence of Zn^{2+}. This is confirmed by the analysis of the electronic density distribution over N9 in the HOMO level (Table 1); in presence of the zinc ion, the donating strength of the nitrogen drastically decreases, in particular, for **1b**, as does the ICT character.

The quantum chemical approach was also used to estimate the change in refractive index upon complexation, Δn, as a function of the number density. Δn was computed from the calculated molecular polarizabilities using the Maxwell–Garnett model[24,25] (see the SI), considering the dye encapsulated in a sol–gel with a concentration of ~1.5 wt % in the dry film. A Δn value of 6×10^{-4} is found, which is in the range of the detection limit of the fiber sensors considered in this work.

Prior to depositing **1** on optical fibers, films of about 100 nm thickness were prepared by drop casting THF solutions of **1** on glass substrates and dipping in aqueous Zn^{2+} solutions of various concentrations. Absorption spectra were recorded every 2 min over a 30 min immersion period. As a control experiment, a film was dipped into pure water. The initial and final spectra are displayed in Figure 1b, while the evolution of the absorption maximum as a function of immersion time in a 2 mol·L^{-1} Zn^{2+} solution is presented in the SI, Figure S8. When dipped in water (and at $t = 0$ in the Zn^{2+} solution), the films show an absorption spectrum similar to that observed in acetone solution, with a shift of ~25 nm (which corresponds to a shift of ~0.1 eV) most probably associated with the difference in dielectric environment. In the presence of Zn^{2+}, the absorption peak gradually shifts hypsochromically from 559 to 521 nm, as a result of the complexation of the zinc ions (no spectral change is observed in the control experiment). This shift (38 nm) is very similar to that measured in solution (33

Table 1. Calculated Spectroscopic Properties of the Free Dye and the Complexes Investigated

	free dye	**1a**·Zn^{2+} CN4	**1a**·Zn^{2+} CN5	**1a**·Zn^{2+} CN6	**1b**·Zn^{2+} CN4	**1b**·Zn^{2+} CN5
λ_{max} (nm)	555	527	530	533	504	510
hypsochromic shift (nm)		28	25	22	51	45
electron density of N9 in HOMO	0.0985	0.0336	0.0431	0.0561	0.0146	0.0239

dx.doi.org/10.1021/jp407460c | J. Phys. Chem. B 2014, 118, 309–314

nm). The long response time (i.e., the shift appears clearly only after 15 min) and the persistence of a shoulder at around 560 nm in the spectrum at t = 30 min are most likely due to the slow diffusion of the ions in the rather thick, hydrophobic organic layer.

The optical fiber sensor consists of a standard silica fiber with a tilted fiber Bragg grating (TFBG) covered with a sensitive layer whose refractive index (real and imaginary parts) changes after the formation of a complex with Zn^{2+}. A fiber Bragg grating is a periodic and permanent modulation of the core refractive index of the optical fiber along the propagation axis that acts as a wavelength-selective filter around the so-called Bragg wavelength.[26] TFBGs couple light between the core and the cladding and present, as a result, a comb-like transmission amplitude spectrum comprising several tens of resonances, each one characterized by its own sensitivity to the surrounding refractive index. The TFBG spectra are directly influenced by the refractive index of the surrounding medium and naturally act as refractometers accurate to 10^{-4} RIU (refractive index unit).[27−29] Specific chemical sensors can be built by using TFBGs covered with a dedicated coating that changes its refractive index when in contact with target chemical species.[30,31] The interrogation length of the TFBG is on the order of the wavelength, typically 1 μm. To obtain maximum response of the TFBG to the refractive index changes of the sensitive coating, its thickness should thus be larger than 1 μm.

The advantage of incorporating the perylene dye in a porous matrix is that the sensitive coating can be thick (a few μm) while keeping the diffusion phenomena rapid. Indeed, in a 1 μm thick layer of pure dye, the very slow diffusion of the ions would result in a very long response time (see the SI, Figure S8). A silica sol−gel was chosen as the host for the dye because its refractive index is close to that of the fiber, in turn enhancing the response.

Figure 4 displays the TFBG amplitude spectra in water and $ZnCl_2$ solution (1 M). The resonance modes in the range 1543−1550 nm are drastically affected after contact with Zn^{2+} ions. This results from the fact that the absorption peak shifts to lower wavelengths, inducing a refractive index change of the layer. The spectra after 2 and 10 min are very similar, indicating a response time on the order of 1 min. We have checked that exposing a pristine sol−gel-coated fiber to a Zn^{2+} aqueous solution leads to no detectable change in the transmission with respect to pure water. The sensor is reversible as it can be regenerated after dipping in an EDTA solution.

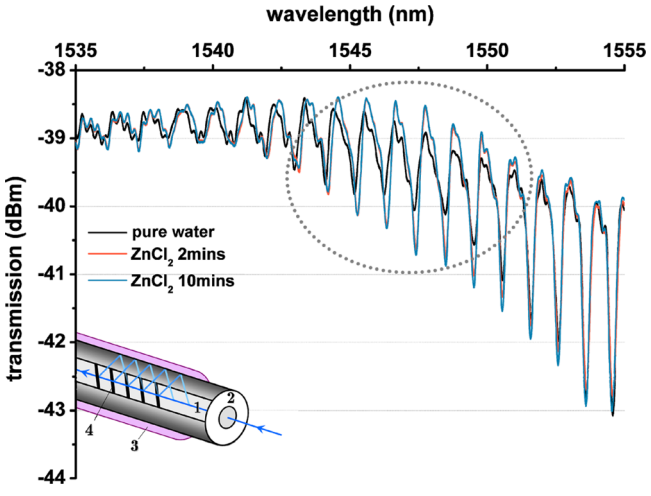

Figure 4. Transmission spectrum of the TFBG in blank solution (black curve) and in contact with Zn^{2+} ions for 2 (orange curve) and 10 min (blue curve). (Inset) Structure of the fiber sensor (1: core; 2: cladding; 3: sol−gel + rylene; 4: TFBG).

CONCLUSION

In summary, we report the synthesis of a chemosensor based on 9-substituted perylene monoimide, which gives highly responsive sensing for Zn^{2+}, both in solution and as a thin layer. The optical response of the chromophore to the Zn^{2+} ions, as explained from quantum chemical calculations, is related to the degree of electronic coupling between the ionophore unit and the perylene unit. The compound was then incorporated in a sol−gel coating, and Zn^{2+} detection in the solid state with fiber sensor technology was also demonstrated. Compound **1** can thus be considered as a promising system for the detection of Zn^{2+} ions, both in organic solutions and in thin film sensors. The design and synthesis of water-soluble Zn^{2+} sensors based on perylene dyes for biological use are in progress.

ASSOCIATED CONTENT

Supporting Information

Fluorescence, FD-MS, ^{1}H NMR, H,H COSY NMR spectra of **1**, thermodynamic parameters from ITC, fluorescence spectra of **1** with different metal ions and associated pictures of the corresponding solutions, optimized geometry of **1** and **1b**·Zn^{2+}, calculated spectroscopic properties of **1** (free and complexed), absorption spectroscopy of **1** as a function of time of exposure to Zn^{2+}, and calculation of the refractive index details. This material is available free of charge via the Internet at http://pubs.acs.org.

AUTHOR INFORMATION

Corresponding Author

*E-mail: claire.tonnele@umons.ac.be.

Author Contributions

‖All authors have given approval to the final version of the manuscript. Z.L. and C.T. contributed equally.

Notes

The authors declare no competing financial interest.

ACKNOWLEDGMENTS

The Mainz−Mons collaboration is supported by the Belgian Science Policy Office (IAP 7/05) and by the European Commission (SUPERIOR). Research in Mons is also supported by the OPTI2MAT Excellence Program of Région Wallonne and FNRS/FRFC. M.S. and D.B. are research associate and research director of the Fonds National de la Recherche Scientifique-FNRS. Financial support of this work by the BASF AG and Deutsche Forschungsgemeinschaft (project SFB 625) is gratefully acknowledged. We also thank Ashlan Musante for her help in preparing this manuscript.

REFERENCES

(1) de Silva, A. P.; Moody, T. S.; Wright, G. D. Fluorescent PET (Photoinduced Electron Transfer) Sensors As Potent Analytical Tools. *Analyst* **2009**, *134*, 2385−2393.

(2) Bissell, R. A.; de Silva, A. P.; Gunaratne, H. Q. N.; Lynch, P. L. M.; Maguire, G. E. M.; Sandanayake, K. R. A. S. Molecular Fluorescent Signalling with 'Fluor−Spacer−Receptor' Systems: Approaches to Sensing and Switching Devices via Supramolecular Photophysics. *Chem. Soc. Rev.* **1992**, *21*, 187−195.

(3) Tal, S.; Salman, H.; Abraham, Y.; Botoshansky, M.; Eichen, Y. Sensitive and Selective Photoinduced-Electron-Transfer-Based Sensing of Alkylating Agents. *Chem.—Eur. J.* **2006**, *12*, 4858−4864.
(4) Chen, X.; Jou, M. J.; Yoon, J. An "Off−On" Type UTP/UDP Selective Fluorescent Probe and Its Application to Monitor Glycosylation Process. *Org. Lett.* **2009**, *11* (10), 2181−2184.
(5) Yukruk, F.; Akkaya, E. U. Modulation of Internal Charge Transfer (ICT) in a Bay Region Hydroxylated Perylenediimide (PDI) Chromophore: A Chromogenic Chemosensor for pH. *Tetrahedron Lett.* **2005**, *46*, 5931−5933.
(6) Bannani, A.; Bobisch, C.; Moeller, R. Ballistic Electron Microscopy of Individual Molecules. *Science* **2007**, *315*, 1824−1828.
(7) Bhosale, S.; Sisson, A. L.; Talukdar, P.; Fuerstenberg, A.; Banerji, N.; Vauthey, E.; Bollot, G.; Mareda, J.; Roeger, C.; Wuerthner, F.; et al. Photoproduction of Proton Gradients with π-Stacked Fluorophore Scaffolds in Lipid Bilayers. *Science* **2006**, *313*, 84−86.
(8) Schmidt-Mende, L.; Fechtenkotter, A.; Müllen, K.; Moons, E.; Friend, R. H.; MacKenzie, J. D. Self-Organized Discotic Liquid Crystals for High-Efficiency Organic Photovoltaics. *Science* **2001**, *293*, 1119−1122.
(9) Wiederrecht, G. P.; Yoon, B. A.; Wasielewski, M. R. High Photorefractive Gain in Nematic Liquid Crystals Doped with Electron Donor and Acceptor Molecules. *Science* **1995**, *270*, 1794−1797.
(10) Langhals, H.; Jona, W. The Identification of Carbonyl Compounds by Fluorescence: A Novel Carbonyl-Derivatizing Reagent. *Chem.—Eur. J.* **1998**, *4*, 2110−2113.
(11) Fan, L.; Xu, Y.; Tian, H. 1,6-Disubstituted Perylene Bisimides: Concise Synthesis and Characterization As near-Infrared Fluorescent Dyes. *Tetrahedron Lett.* **2005**, *46*, 4443−4447.
(12) Yan, P.; Holman, M. W.; Robustelli, P.; Chowdhury, A.; Ishak, F. I.; Adams, D. M. Molecular Switch Based on a Biologically Important Redox Reaction. *J. Phys. Chem. B* **2005**, *109*, 130−137.
(13) Che, Y.; Datar, A.; Balakrishnan, K.; Zang, L. Ultralong Nanobelts Self-Assembled from an Asymmetric Perylene Tetracarboxylic Diimide. *J. Am. Chem. Soc.* **2007**, *129*, 7234−7235.
(14) He, X.; Liu, H.; Li, Y.; Wang, S.; Li, Y.; Wang, N.; Xiao, J.; Xu, X.; Zhu, D. Gold Nanoparticle-Based Fluorometric and Colorimetric Sensing of Copper(II) Ions. *Adv. Mater.* **2005**, *17*, 2811−2815.
(15) Lee, B. Review of the Present Status of Optical Fiber Sensors. *Opt. Fiber Technol.* **2003**, *9*, 57−79.
(16) Becke, A. D. Density-Functional Thermochemistry. III. The Role of Exact Exchange. *J. Chem. Phys.* **1993**, *98*, 5648−5652.
(17) Hay, P. J.; Wadt, W. R. Ab Initio Effective Core Potentials for Molecular Calculations. Potentials for the Transition Metal Atoms Sc to Hg; Potentials for Main Group Elements Na to Bi; Potentials for K to Au Including the Outermost Core Orbitals. *J. Chem. Phys.* **1985**, *82* (270), 284−299.
(18) Tomasi, J.; Mennucci, B.; Cancès, E. The IEF Version of the PCM Solvation Method: An Overview of a New Method Addressed to Study Molecular Solutes at the QM Ab Initio Level. *J. Mol. Struct.: THEOCHEM* **1999**, *464*, 211−226.
(19) Frisch, M. J.; Trucks, G. W.; Schlegel, H. B.; Scuseria, G. E.; Robb, M. A.; Cheeseman, J. R.; Scalmani, G.; Barone, V.; Mennucci, B.; Petersson, G. A.; et al. *Gaussian 09*, revision A.02; Gaussian, Inc.: Wallingford, CT, 2009.
(20) 9-bromo-PMI was synthesized following procedures reported in: Li, C.; Wonneberger, H. Perylene Imides for Organic Photovoltaics: Yesterday, Today, and Tomorrow. *Adv. Mater.* **2012**, *24*, 613−636.
(21) Geerts, Y.; Quante, H.; Platz, H.; Mahrt, R.; Hopmeier, M.; Böhm, A.; Müllen, K. Quaterrylenebis(dicarboximide)s: Near Infrared Absorbing and Emitting Dyes. *J. Mater. Chem.* **1998**, *8*, 2357−2369.
(22) Bjelic, S.; Jelesarov, I. A Survey of the Year 2007 Literature on Applications of Isothermal Titration Calorimetry. *J. Mol. Recognit.* **2008**, *21*, 289−311.
(23) Qvortrup, K.; Bond, A. D.; Nielsen, A.; McKenzie, C. J.; Kilsa, K.; Nielsen, M. B. Perylenediimide-Metal Ion Dyads for Photo-Induced Electron Transfer. *Chem. Commun.* **2008**, *17*, 1986−1988.
(24) Maxwell Garnett, J. C. Colours in Metal Glasses and in Metallic Films. *Philos. Trans. R. Soc. London, Ser. A* **1904**, *203*, 385−420.
(25) Choy, T. C. *Effective Medium Theory: Principles and Applications*; Oxford University Press: New York, 1999.
(26) Kersey, A. D.; Davis, M. A.; Patrick, H. J.; LeBlanc, M.; Koo, K. P.; Askins, C. G.; Putnam, M. A.; Friebele, E. J. Fiber Grating Sensors. *J. Lightwave Technol.* **1997**, *15*, 1442−1463.
(27) Laffont, G.; Ferdinand, P. Tilted Short-Period Fibre-Bragg-Grating-Induced Coupling to Cladding Modes for Accurate Refractometry. *Meas. Sci. Technol.* **2001**, *12*, 765−770.
(28) Caucheteur, C.; Mégret, P. Demodulation Technique for Weakly Tilted Fiber Bragg Grating Refractometer. *IEEE Photonics Technol. Lett.* **2005**, *17*, 2703−2705.
(29) Chan, C.-F.; Chen, C.; Jafari, A.; Laronche, A.; Thomson, D. J.; Albert, J. Optical Fiber Refractometer Using Narrowband Cladding-Mode Resonance Shifts. *Appl. Opt.* **2007**, *46*, 1142−1149.
(30) Baldini, F.; Brenci, M.; Chiavaioli, F.; Giannetti, A.; Trono, C. Optical Fibre Gratings As Tools for Chemical and Biochemical Sensing. *Anal. Bioanal. Chem.* **2011**, *402*, 109−116.
(31) Debliquy, M.; Renoirt, J.-M.; Caucheteur, C.; Mégret, P.; Olivier, M.-G. Volatile Organic Compounds Detection with Tilted Fiber Bragg Gratings Coated by ZnO Nanoparticles. *Proceedings SPIE Photonics Europe*; 2012, paper n° 8439-92.